

Development of SPACE Code for Thermal-Hydraulic Analysis of Ocean Nuclear Reactors

Byoung Jae Kim¹, Seung-Wook Lee², and Kyung Doo Kim²

¹School of Mechanical Engineering, Chungnam National University

²Reactor System Safety Research Division, Korea Atomic Energy Research Division

E-mail: bjkim@cnu.ac.kr

1. Introduction

Various efforts have been made to develop thermal-hydraulic codes for ocean nuclear reactors based on RETRAN [1], RELAP5 [2, 3], and MARS [4].

Recently, the SPACE code has been modified for ocean nuclear reactors. This paper reports some results of conceptual problems to demonstrate the capability of system analysis of ocean nuclear reactors. In particular, the effects of the rotational acceleration are presented.

2. Code development

The conservation equations for scalar properties remain unchanged under the change of the frame, i.e., frame indifferent. However, fictitious force terms appear to the momentum equation. The two-fluid momentum equation for phase k in the non-inertial frame of reference is written as

$$\begin{aligned} & \frac{\partial}{\partial t}(\alpha_k \rho_k \mathbf{u}_k) + \nabla \cdot (\alpha_k \rho_k \mathbf{u}_k \mathbf{u}_k) \\ & = -\alpha_k \nabla p_k + \nabla \cdot [\alpha_k (\boldsymbol{\tau}_k + \boldsymbol{\tau}_k^{\text{Re}})] + \alpha_k \rho_k \mathbf{g} \quad , \quad (1) \\ & + (p_{ki} - p_k) \nabla \alpha_k + \mathbf{u}_{ki} \Gamma_k + \mathbf{M}_{ik} - \nabla \alpha_k \cdot \boldsymbol{\tau}_{ki} \\ & - \alpha_k \rho_k [\ddot{\mathbf{R}} + \dot{\boldsymbol{\Omega}} \times \mathbf{r} + 2\boldsymbol{\Omega} \times \mathbf{u}_k + \boldsymbol{\Omega} \times (\boldsymbol{\Omega} \times \mathbf{r})] \end{aligned}$$

where $\ddot{\mathbf{R}}$ and $\dot{\boldsymbol{\Omega}}$ are the linear acceleration vector and rotational vector, respectively, of the moving coordinates with regard to the fixed coordinates [5]. For one-dimensional adiabatic flow, Eq. (1) can be written as

$$\begin{aligned} & \frac{\partial}{\partial t}(\alpha_k \rho_k u_k) + \frac{\partial}{\partial x}(\alpha_k \rho_k u_k u_k) \\ & = -\alpha_k \nabla p - F_{ik} - F_{wk} + \alpha_k \rho_k g_x \quad (2) \\ & - \alpha_k \rho_k [\ddot{\mathbf{R}} + \dot{\boldsymbol{\Omega}} \times \mathbf{r} + \boldsymbol{\Omega} \times (\boldsymbol{\Omega} \times \mathbf{r})]_x \end{aligned}$$

where $[\cdot]_x$ denotes the main pipe direction. In Eq. (2), the last term consists of the linear acceleration, Euler force, and centrifugal force. The Coriolis effect has been neglected.

There are a number of ways to express the three-dimensional rotation. Of them, the intrinsic rotation with Tait-Bryan angles is adopted in the SPACE code.

The geometrical parameters such as inclined angle and azimuthal angle for each component are updated while a whole reactor system rotates. The thermal-hydraulic options and models for each component are also updated according to the dynamic inclined angle.

3. Rotation test

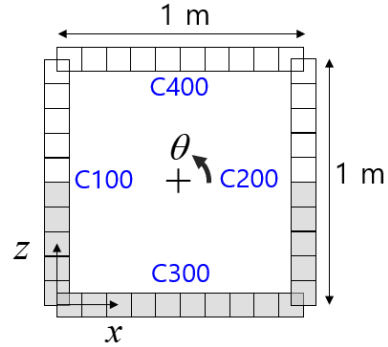


Fig. 1 Square manometer half filled with water

Figure 1 shows the square manometer. Each pipe is 1 m in length and 0.1 m in diameter. Initially, the water is half filled in the manometer at a saturation pressure of 100 bar. Figure 2 shows the water lengths in left and right pipes as the manometer rotates in the counter-clockwise direction as $\theta = A \sin(2\pi t / T)$. Since the rotation speed is low, the gravity direction is the dominant factor to determine the water position.

Figure 3 shows the result when the rotation angle slowly increases up to 60° and come to a standstill. The rotation speed is $1^\circ/\text{s}$ for first 60 s. Thus, until 60 s, the time can be interpreted as the rotation angle. The left pipe becomes full and the right pipe becomes empty. Figure 4 shows the result when the manometer rotates by 360° . The predictions are excellent. These results demonstrate well working of head according to rotation.

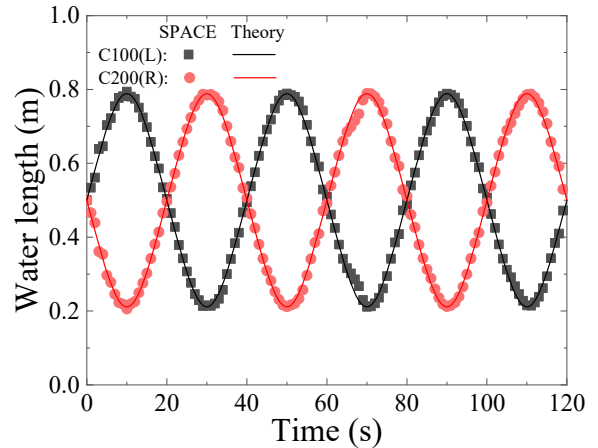


Fig. 2 Collapsed water length: $A = 30^\circ$ and $T = 40$ s.

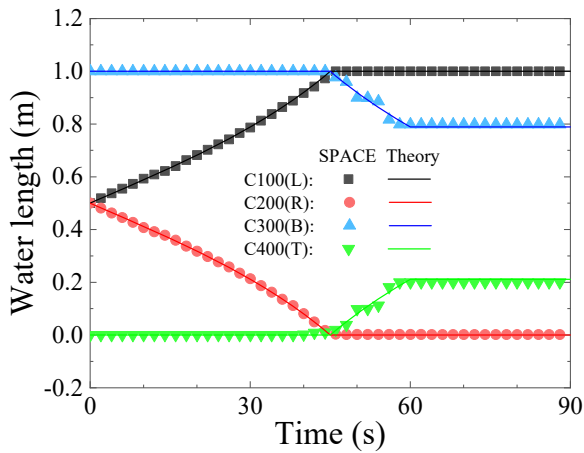


Fig. 3 Water length for the rotation up to 60°

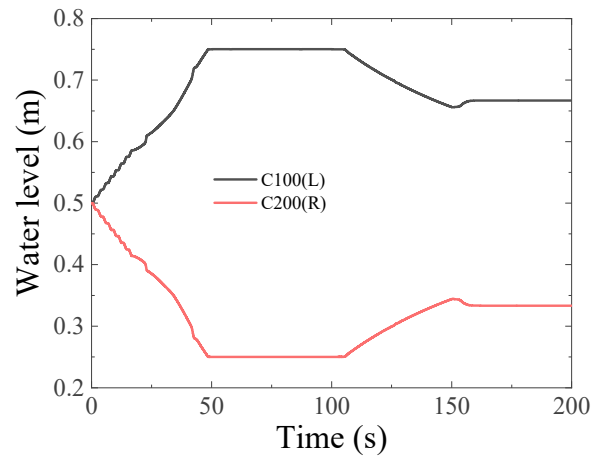


Fig. 5 Results for both horizontal and vertical accelerations

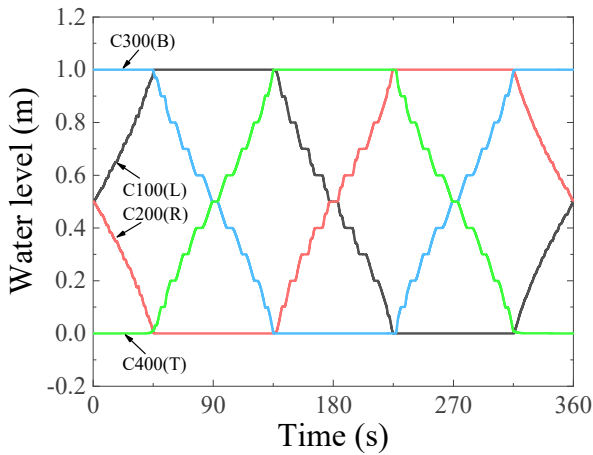


Fig. 4 Water length for the rotation up to 360°

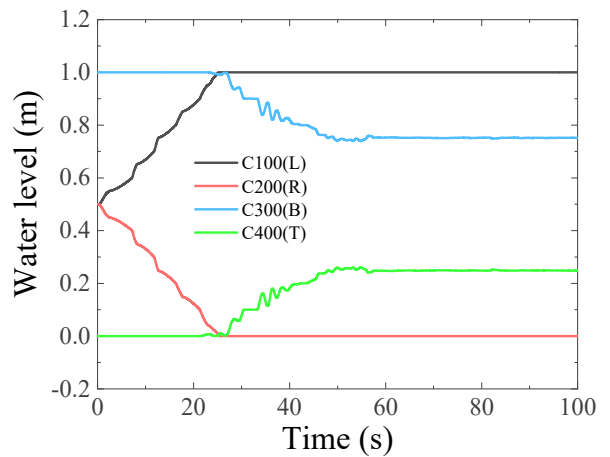


Fig. 6 Results when a horizontal acceleration is increased up to 19.62 m²/s.

4. Linear acceleration test

Figure 5 shows the result when a horizontal acceleration is increased up to 4.905 m²/s for first 50 s and lasts until 100 s. Additionally, a vertical acceleration is increased up to 4.905 m²/s for the next 50 s and lasts until 200 s. The waver levels are well predicted. Figure 6 shows the result when a horizontal acceleration is increased up to 19.62 m²/s for 50 s such that the water reaches the top pipe.

5. Rotational acceleration test: centrifugal force

The fluid in the rotating system experiences the centrifugal force. Figure 7 shows the square manometer rotating about the z axis, i.e., $\Omega = \omega \mathbf{k}$.

Figure 8 and 9 show the water levels for $\omega = 90^\circ / \text{s}$ and $\omega = 360^\circ / \text{s}$, respectively. For the latter case, the centrifugal force is so large that the water reaches the top pipe.

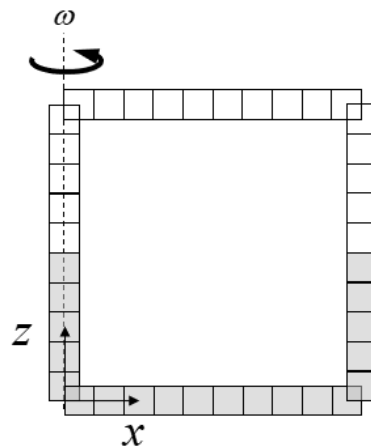


Fig. 7 Square manometer rotating about the z axis

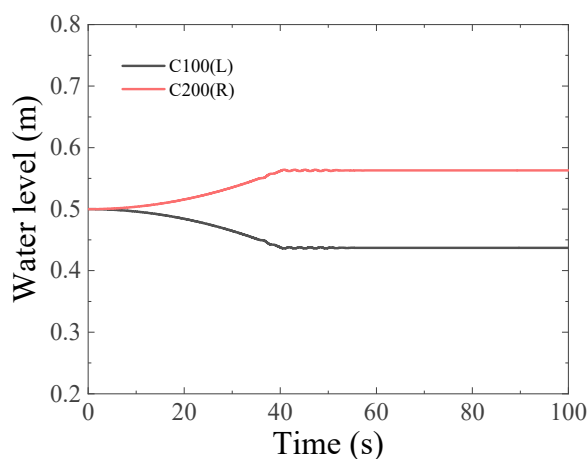


Fig. 8 Result for $\omega = 90^\circ / s$

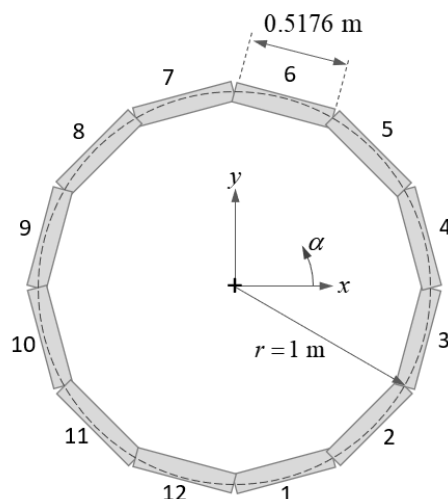


Fig. 10 Horizontal torus

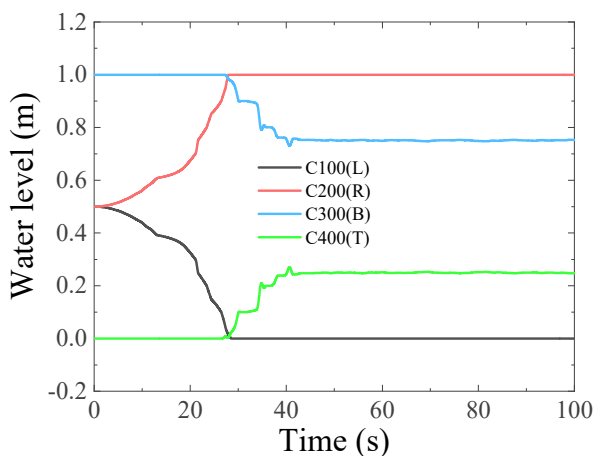


Fig. 9 Result for $\omega = 360^\circ / s$

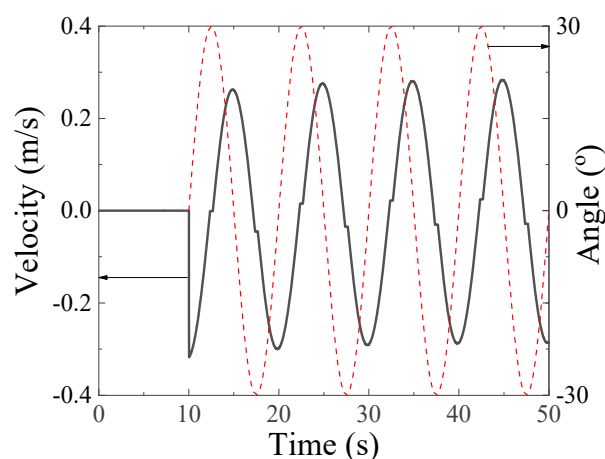


Fig. 11 Result of rotationally oscillating horizontal torus

6. Rotational acceleration test: Euler force

Figure 10 shows a horizontal torus with a radius of 1 m. Twelve identical pipes are connected to form the torus. Each pipe has a diameter of 0.1 m and a length of 0.5176 m. Initially, the water is half filled in the torus. The torus is rotating about the z axis as $\boldsymbol{\Omega} = \alpha \mathbf{k} = A \sin(2\pi t / T) \mathbf{k}$, where A is 30° and the period is $T=10$ s. In this situation, the water experiences only the Euler force due to the angular acceleration. Figure 11 shows the result. The torus oscillation starts at 10 s. One can see that there is a phase difference of 90° between the oscillation and water velocity. The reason is that the Euler force is proportional to the time derivative of the angular velocity. In Eq. (2), the term $-\alpha_k \rho_k \dot{\boldsymbol{\Omega}} \times \mathbf{r}$ accounts for the Euler force. Although not shown here, at every pipe, the void fractions remain at 0.5.

6. Conclusions

The SPACE code has been modified to include the effects of linear and rotational accelerations. The simulation results demonstrated the capability of the SPACE code for ocean nuclear reactor. The code will be extended to three-dimensional flow based on the cross-flow junctions.

ACKNOWLEDGEMENTS

This work was supported by the National Research Foundation of Korea (NRF) funded by Ministry of Science and ICT (Grant No. NRF-2016M2B2A9A02944972). This work was supported by the National Research Foundation of Korea (NRF) funded by Ministry of Science and ICT (Grant No. NRF-2017M2A8A4016738).

REFERENCES

1. Ishida, I., et al., *Thermal-hydraulic behavior of a marine reactor during oscillations*. Nuclear Engineering and Design, 1990. **120**(2): p. 213-225.
2. Yan, B.H. and L. Yu, *The development and validation of a thermal hydraulic code in rolling motion*. Annals of Nuclear Energy, 2011. **38**(8): p. 1728-1736.
3. Mesina, G.L., et al., *Modeling Moving Systems with RELAP5-3D*. Nuclear Science and Engineering, 2016. **182**: p. 83-95.
4. Beom, H.-K., et al., *Verification and improvement of dynamic motion model in MARS for marine reactor thermal-hydraulic analysis under ocean condition*. Nuclear Engineering and Technology, 2019. **51**(5): p. 1231-1240.
5. Kim, B.J., et al., *Two-fluid equations for two-phase flows in moving systems*. Nuclear Engineering and Technology, 2019. **51**(6): p. 1504-1513.